

Effect of local pipe bends on pump performance of a small air-lift system in transporting solid particles

Hitoshi Fujimoto ^{a,*}, Shio Murakami ^b, Ayumu Omura ^b, Hirohiko Takuda ^a

^a *Department of Energy Science and Technology, Graduate School of Energy Science, Kyoto University, Yoshida-Honmachi, Sakyo-ku, Kyoto 606-8501, Japan*

^b *Graduate School of Energy Science, Kyoto University, Yoshida-Honmachi, Sakyo-ku, Kyoto 606-8501, Japan*

Received 3 June 2003; accepted 18 February 2004

Available online 20 May 2004

Abstract

The pump performance of a small air-lift system in transporting solid particles is investigated experimentally. Three types of riser pipe were used to examine the effect of local bends of riser pipes on the flow characteristics of a three-phase air–water–solid particles mixture. Two of them were locally S-shaped either below or above a gas injector. The other was vertically straight. Alumina particles of 3 or 5 mm diameter were used as solid particles. It is indicated that the pump performance is appreciably reduced when the pipe bend is above the gas injector. The critical condition under which solid particles are vertically lifted is discussed from a practical viewpoint. In addition, the particle motion in the region of a pipe bend is investigated by photographic observations.

© 2004 Elsevier Inc. All rights reserved.

Keywords: Air-lift pump; Gas–water–solid particles three-phase mixture; Critical condition; Pump performance; Local pipe bends

1. Introduction

The air-lift pump is a device designed to transport liquid or slurries of small solid particles vertically upward along a riser pipe (Khalil et al., 1999; Sekoguchi et al., 1981). The pump consists of an air compressor, an air injector, and a vertical riser pipe that is open at both ends (see Fig. 1). Compressed air is injected into the riser pipe through the air injector, with buoyancy driving the air bubbles upward within the liquid. The bubbles soon coalesce to an extent that their cross-sectional diameter is almost the same as the pipe diameter. As a consequence, the liquid and the large air bubbles appear alternately along the pipe. Such bubble motion induces upward liquid flow, and thus liquid is transported along the pipe.

The air-lift pump can also be used in conveying relatively large solid particles together with liquid (Kato et al., 1975; Weber and Dedegil, 1976; Shaw, 1993; Yoshinaga and Sato, 1996; Hatta et al., 1999; Fujimoto et al., 2003). In this case, the driving mechanism for

conveying solid particles is the frictional drag force exerted by the surrounding liquid or liquid/air mixture. Since the upward drag force on the particles must be larger than the gravitational force, a critical value exists, at which the solid particles can be lifted. In general, the pump efficiency of air-lift pumps is relatively small compared to mechanical pumps. Thus, serious attention needs to be paid to this critical condition when designing air-lift pumps for transporting solid particles.

From the standpoint of pump performance, it is desirable for the riser pipe to be vertically straight. If the riser pipe has local bends, the pump performance is reduced due to the loss of momentum of liquid at each bend. The riser pipe may also become clogged with the solid particles at each bend. In principle, the presence of local bends will not improve the pump performance. To date, experimental and analytical studies of the performance of air-lift pumps for conveying relatively large solid particles have been concerned with vertical straight riser pipes (Kato et al., 1975; Weber and Dedegil, 1976; Yoshinaga and Sato, 1996; Hatta et al., 1999; Fujimoto et al., 2003).

Despite their apparent deficiencies, the utilization of locally bent or flexible riser pipes is inevitable in actual

* Corresponding author. Tel.: +81-75-753-5419; fax: +81-75-753-5428.

E-mail address: h-fujimoto@energy.kyoto-u.ac.jp (H. Fujimoto).

Nomenclature

C_D	drag coefficient	j_s	superficial velocity of solid phase, m/s
d_s	particle diameter, m	L_s	vertical distance between water level and the bottom of riser pipe defined in Fig. 3(a), m
g	gravitational acceleration, m/s ²	t	time, s
j_{Ga}	gas volumetric flux (superficial velocity) reduced to the atmospheric state, m/s	u_L	velocity of liquid phase, m/s
j_L	superficial velocity of liquid phase, m/s	u_s	velocity of solid phase, m/s
$j_{L,min}$	critical flux (or critical superficial velocity) of water for conveying a solid particle in an air-lift pump, m/s	ρ_L	liquid density, kg/m ³
		ρ_s	material density of solid particles, kg/m ³

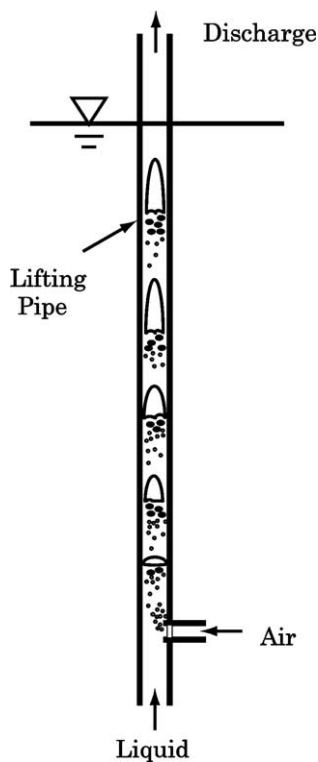


Fig. 1. Schematic of air-lift pump.

use. For example, deep-sea mineral resources may be lifted in the future by means of air-lift pumps in which the riser includes a section of flexible pipe. However, few studies have focused on the consequences of local pipe bends in air-lift pumps used for conveying solid particles. The performance of locally bent air-lift pumps remains unexplored.

In the present study, the flow characteristics in a small air-lift pump for transporting solid particles is investigated in detail. The main purpose is to examine the effect of local pipe bends on the total performance of the air-lift pump. To this end, three types of lifting pipes

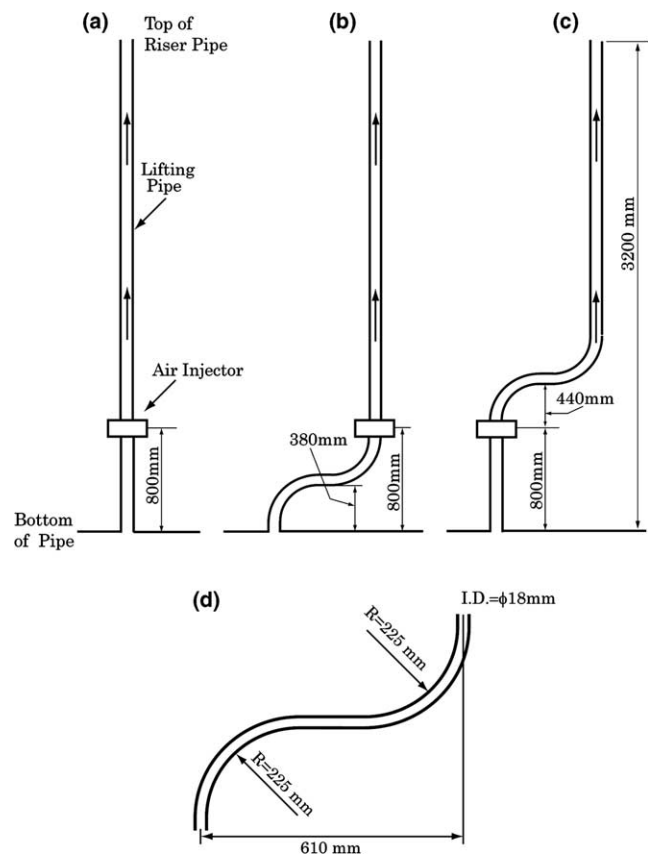


Fig. 2. Dimensions of riser pipes used in the present study.

are prepared, as shown in Fig. 2. One lifting pipe is vertically straight. The other two risers are locally S-shaped either below or above the gas injector. Alumina particles of 3 or 5 mm diameter are used as solid particles. The pump performance and the critical condition under which solid particles are lifted vertically are discussed with reference to the experimental results. In addition, the particle motion in the region of a pipe bend is investigated by photographic observations.

2. Experiments

Fig. 2(a)–(c) depict the three types of riser pipes used in the present experiments. For convenience, these riser pipes will be referred to as pipes A, B, and C, respectively. Riser pipe A consists of a straight pipe (made of transparent plastic) and an air injector. The other two riser pipes (B and C) consist of straight pipes, the air injectors, and S-shaped glass pipes whose dimensions are shown in Fig. 2(d). It should be noted that the local radius of curvature of the S-shaped pipe is 235 ± 10 mm. The height of the lifting pipes is 3200 mm and the internal diameter of the pipes is 18 mm for all cases. The gas injection point is set 800 mm above the bottom of the pipes.

Fig. 3(a) shows a schematic of the experimental setup. Since, except for the lifting pipes, the experimental apparatus and the measurement procedure are almost the same as those in our previous study (Fujimoto et al., 2003), they are briefly described here. The air-lift pump consists of a reservoir, a particle feeder, a suction box, a riser pipe, an air injector, an air compressor, and an air separator set at the top of the riser pipe. During experimentation, the water level in the reservoir was maintained at a preset height. The vertical distance, L_s , between the water level and the bottom of the riser pipe was varied from 1925 to 2433 mm.

The particle feeder supplied solid particles to the suction box located at the bottom of the riser pipe. Alumina particles of 3 or 5 mm diameter were used as the solid particles. The material density, ρ_s , of alumina is 3600 kg/m^3 .

The gas mass flow controller regulated the volume rate of the supplied air. The gas volumetric flux (superficial velocity), j_{Ga} , reduced to the atmospheric state was in the range of $0 < j_{Ga} \leq 3.27 \text{ m/s}$. The measurement accuracy of j_{Ga} was within $\pm 0.03 \text{ m/s}$. Air was injected into the riser pipe through four holes of 5 mm diameter, as shown in Fig. 3(b). The effect of the gas injection method, including hole diameter and number of holes, on the pump performance has been previously investigated (Fujimoto et al., 2003). The present gas injection method is based on that study.

Experiments were carried out under stable pump operating conditions. That is, the mean flow rates of the injected air and solid particles were maintained at preset values, and the mean flow rate of discharged water was kept nearly constant. The superficial velocity of discharged water, j_L , was determined by the volume of discharged water, the sampling time, and the cross-sectional area of the riser pipe. The superficial velocity of discharged solid particles, j_s , was measured similarly. The sampling times employed were 10 or 20 s. The measurement uncertainties of j_L and j_s were within ± 0.01 and $\pm 0.001 \text{ m/s}$, respectively.

3. Results and discussion

3.1. Performance curves of a small air-lift pump containing local bends

Fig. 4 depicts typical pump curves for air–water two-phase mixtures. The type of riser pipe and the vertical distance L_s from the bottom of the riser pipe to the water level in the reservoir were varied as parameters. Since the buoyancy of the air in the liquid provides the driving force for lifting the liquid, the performance of the pump is highly dependent on the amount of injected air. In all cases, the pump curves show similar trends. The superficial velocity of the discharged water increased with the volumetric flux of the injected air, eventually reaching a maximum value, and then decreasing slightly. The peak may be due to a change of flow patterns from slug flow to churn-turbulent flow and an increase of momentum loss due to wall friction. In addition, the discharged water flux is smaller for lower L_s , because the hydraulic head between the top of the riser pipe and the water level in the reservoir is smaller.

The discharged water flux in the straight riser pipe A is larger than that in the locally bent risers B and C. Since the total length of pipe A is shorter than other pipes, the head loss due to the pipe wall friction becomes smaller. Further, the head loss is greater in B and C due to the local pipe bends. The pump performance is thus highest for pipe A.

The difference is small between the water flux values in riser pipes A and B, suggesting that the momentum losses due to the pipe bends and the wall friction of the long pipe length are very small, when the S-shaped portion of the pipe contains only water. On the other hand, the water flux in pipe C is appreciably smaller than that in A or B. In C air is injected prior to the bend, signifying a mixture of air and water flowing in the S-shaped portion of the riser. Observation with the naked eyes reveals that the air and water flow separately in the middle part of the S-shaped pipe where the flow path is horizontal. The water flows in the lower part of the circular cross-section of the pipe, while the air moves in the upper part. The flow pattern changes from separated flow to slug or churn flow as the flow path shifts from the horizontal to the vertical region of the pipe. This may reduce the pump performance. Placing the pipe bend above the gas injector is clearly unsuitable.

Fig. 5(a)–(f) depicts the relationship between the injected gas flux and the flux of resultant discharged water for the gas–liquid–solid particles three-phase mixtures. The dotted lines show the critical water flux, $j_{L,\min}$, for lifting a single solid particle, as it will be described in later subsection. The particles are transported only if relatively large gas fluxes are injected into the riser pipes. As expected, larger gas flux is needed to increase the discharged particle flux. The pump performance in

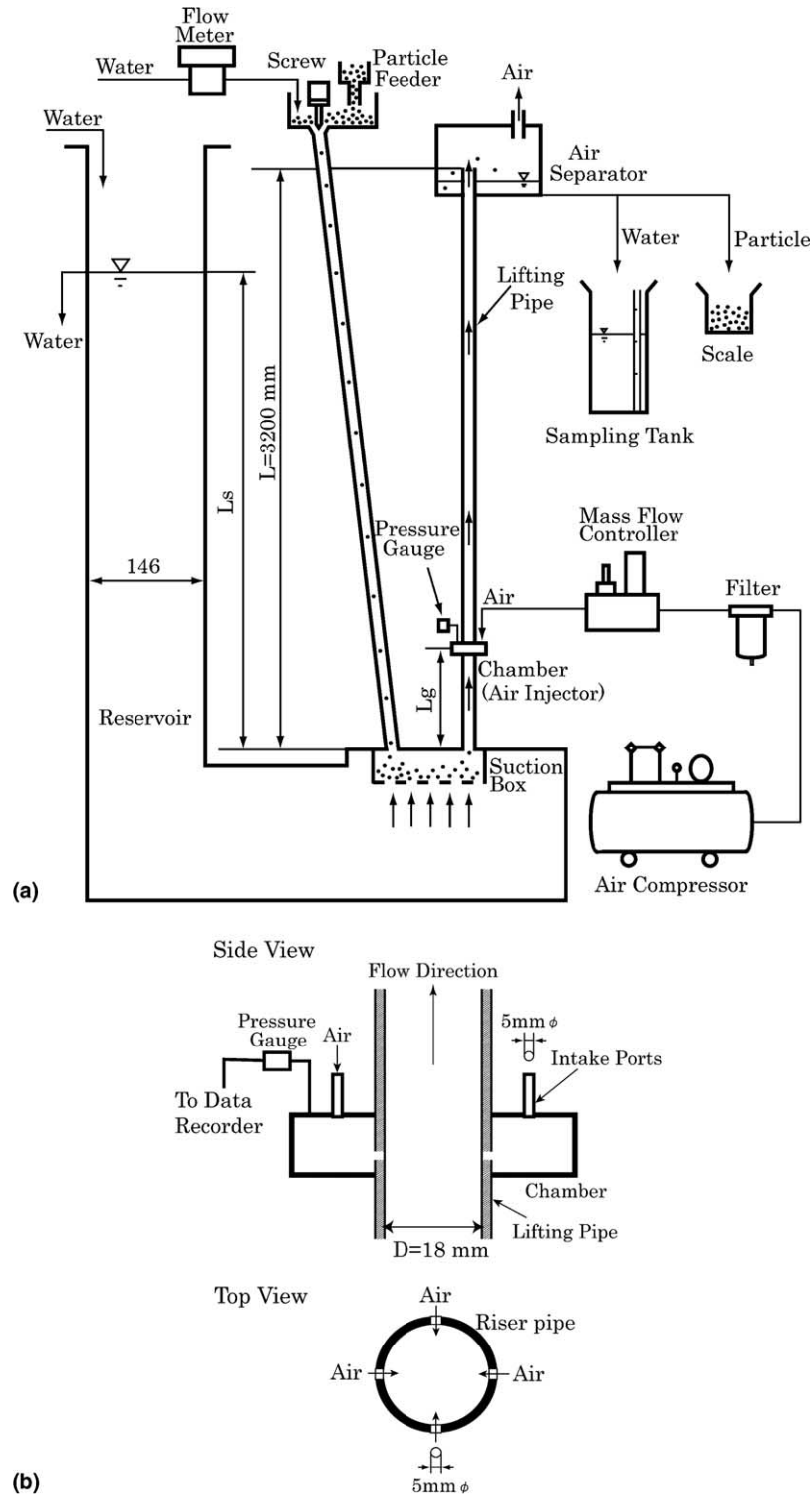


Fig. 3. Experimental apparatus.

transporting alumina particles is poor in the present pump system. The performance curves for three-phase flows are very similar to those for two-phase flows. The water flux for three-phase flow is always less than that for the case of two-phase flow ($j_s = 0$ m/s), because the momentum transfer occurs from the liquid to the solid

phase. The water flux at a given gas flux decreases with an increase in the flux of solid particles. In addition, the performance curves in transporting solid particles show the similar trends to those obtained by using straight pipes (Yoshinaga and Sato, 1996; Fujimoto et al., 2003).

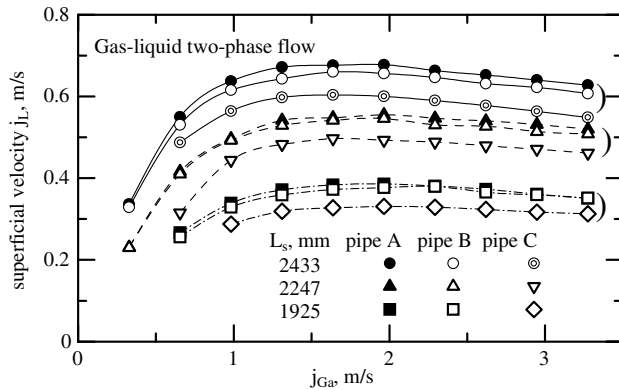


Fig. 4. Pump performance for air–water two-phase flows.

It is worth noting that the flows in the riser pipes are essentially chaotic and unsteady, because the liquid and the air slugs move up alternately in the riser pipe above the gas injector (Sekoguchi et al., 1981). Such unsteady motion of the mixture flow gives rise to a fluctuation of pressure in the chamber. The pressure gauge set in the chamber can capture the variation of air pressure with a time resolution of 5 ms. The variation of pressure was measured under various conditions and a frequency analysis was performed to show the unsteady nature of the flows. Fig. 6 shows the results of frequency analysis. The sampling time was approximately 40 s. Samples of 8192 pressure data taken at every 5 ms were used to calculate the power spectrum. The maximum intensity is set to 100 for each figure. It appears that the frequency profile of the pressure depends on the gas flux. A relatively strong periodicity appears at around 2 Hz for

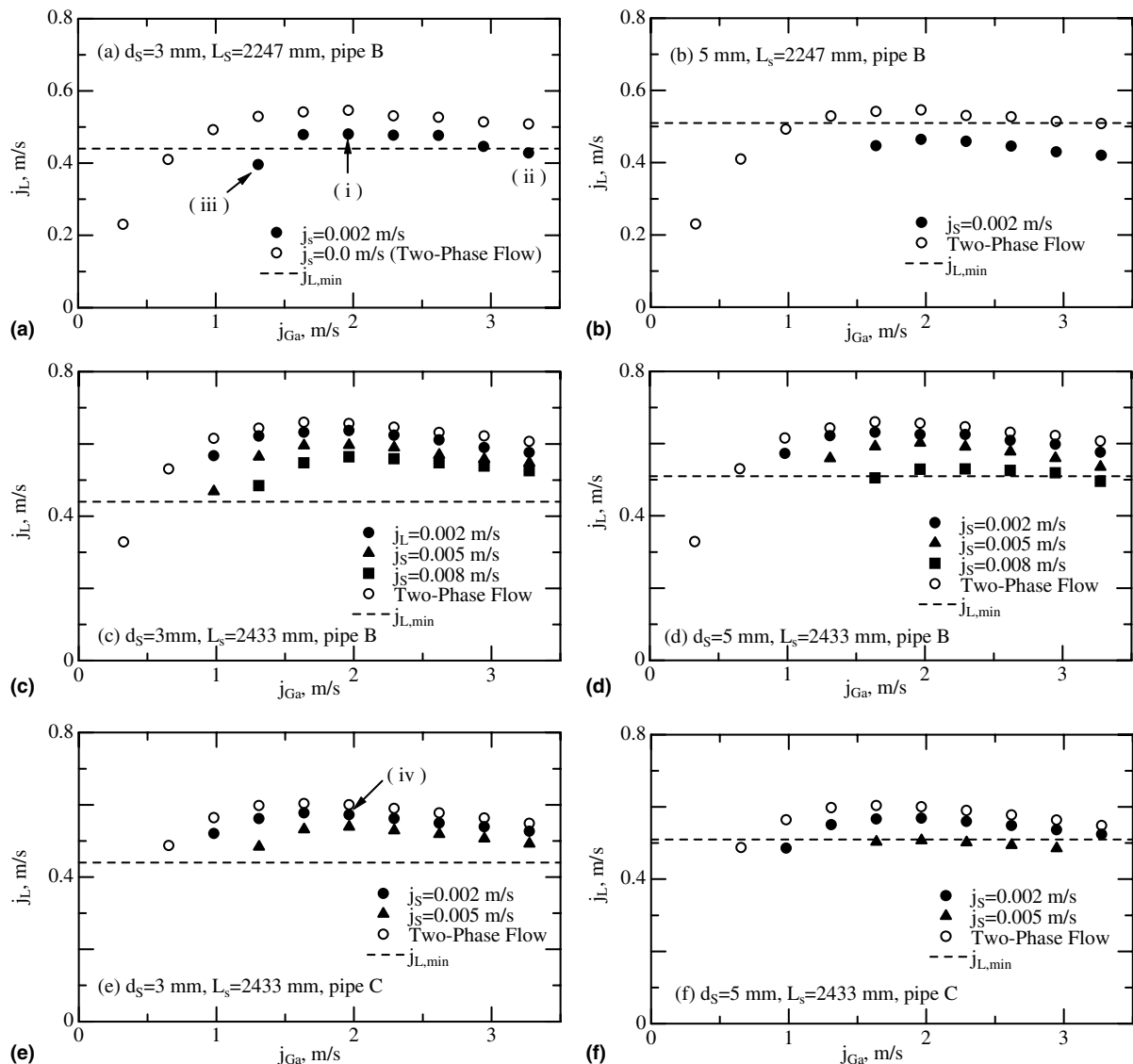


Fig. 5. Pump performance for air–water–solid particles three-phase flows.

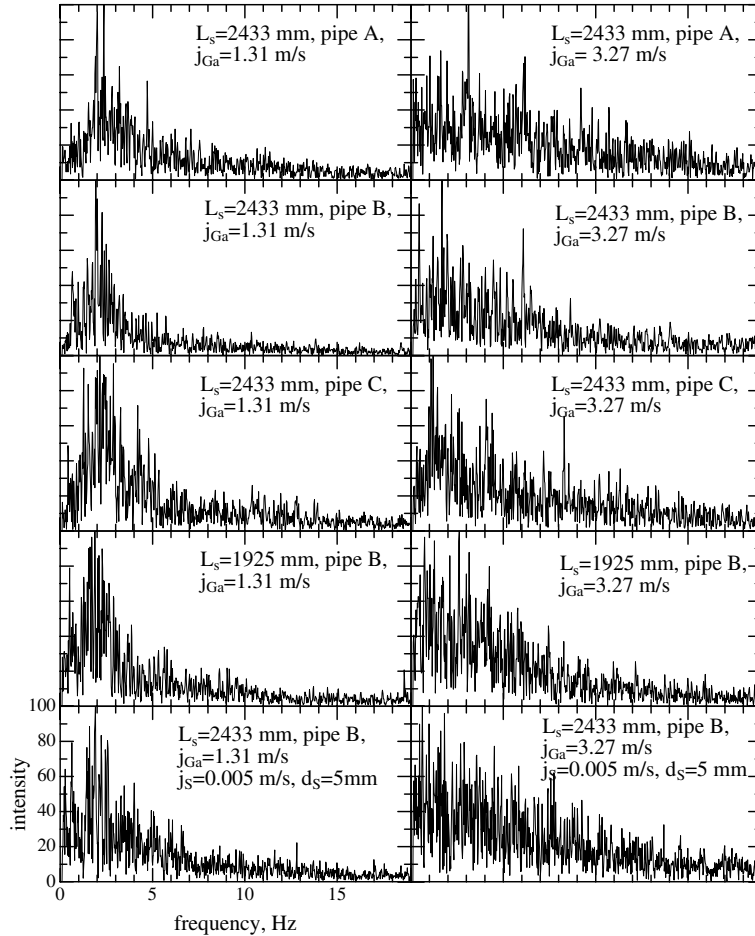


Fig. 6. Frequency analysis of pressure in the chamber.

$j_{Ga} = 1.31$ m/s, but is not seen when $j_{Ga} = 3.27$ m/s. This might be due to the flow patterns in the riser pipes. The flow pattern is slug flow for $j_{Ga} = 1.31$ m/s, while it shows churn-turbulent flow for $j_{Ga} = 3.27$ m/s. The effects of other factors (such as L_s , the type of pipe, and the presence of particles) are not apparent, despite the authors' expectation that these factors, particularly the type of pipe, might affect the flow characteristics in the riser pipes. As previously explained, in pipe C, the flow pattern sharply changes between slug/churn-turbulent flow and separated flow in the S-shaped portion of the pipe. In pipes A and B, it does not occur. Therefore, the flow characteristics are obviously different, depending on the type of pipe. However, any appreciable features cannot be seen in the frequency profile of the pressure in the chamber for pipe C.

3.2. Critical conditions for vertically conveying a solid particle

In designing an air-lift system utilized for conveying relatively large solid particles, whether the critical conditions for conveying solid particles exist is a very

important consideration. In the riser pipes of air-lift pump, solid particles are conveyed vertically upward against the gravity through the drag force exerted by the surrounding liquid or air/liquid mixture. If the drag force on the particles in the upward direction is less than the gravitational force, the particles will not rise.

Consider the momentum equation for a single solid particle in the liquid, taking into account the drag force between the solid and the liquid, and gravity (Fujimoto et al., 2003):

$$\frac{Du_s}{Dt} = -g \frac{\rho_s - \rho_L}{\rho_s} + \frac{3}{4d_s} C_D \frac{\rho_L}{\rho_s} |u_L - u_s| (u_L - u_s) \quad (1)$$

in which t , g , u_L , u_s , d_s , ρ_L and C_D are the time, the gravitational acceleration, the velocities for liquid and solid phases, the diameter of the solid particle, the liquid density, and the drag coefficient, respectively. The solid particle is essentially transported upward in the liquid if $Du_s/Dt \geq 0$. Thus, the critical liquid velocity for transporting a single solid particle very slowly ($u_s \sim 0$) is given by:

$$u_{L,cri} \sim \sqrt{\frac{4d_s g}{3C_D} \frac{\rho_s - \rho_L}{\rho_L}} \quad (2)$$

Since the types of liquid and solid are fixed in the present experiments, the critical liquid velocity depends on the particle diameter alone. The correlation suggests that the dominant factor for transporting solid particles is the velocity of the surrounding fluid, although the ideal motion of a single particle in uniform liquid flow is essentially different from the unsteady particle motion in the air-lift pump.

From this standpoint, the critical condition, on which a single solid particle is conveyed, was measured experimentally as follows. At first, the riser pipe was filled with quiescent water and particles were injected through the suction box located at the bottom of the riser pipe. Then, very small amounts of air were injected into the riser pipe through the injector. The amount of injected air was increased gradually until only one solid particle moved upward very slowly in the riser pipe. The moving rate of particles in the vertical pipe below the gas injector was smaller than that above the gas injector. Therefore, the critical condition was dependent upon the flow characteristics of water below the gas injector.

Table 1 lists the critical conditions obtained. The critical water flux (or critical superficial velocity), $j_{L,min}$, was 0.44 and 0.51 m/s for particles of 3 and 5 mm diameters, respectively. As expected, the critical water flux, $j_{L,min}$, was dependent only upon the particle size, remaining independent of the type of riser pipe and the water level in the reservoir. The particles were not conveyed for the experimental condition $L_s = 1925$ mm.

Incidentally, the right hand side of Eq. (2) coincides with the terminal velocity (settling velocity) of particles in a quiescent liquid. The authors measured the terminal velocity in the case where a single particle descends in quiescent water in a 2 m height of rectangular duct, as shown in Fig. 7(a), by means of a conventional photographic technique. The measured terminal velocity was 0.49 m/s for $d_s = 3$ mm, and 0.64 m/s for $d_s = 5$ mm, respectively. The corresponding drag coefficient was approximately 0.42 in both cases. These terminal velocities were appreciably larger than the critical water flux, $j_{L,min}$.

Table 1

Critical condition on which a single solid particle is conveyed

d_s , mm	j_{Ga} , m/s	j_L , m/s	L_s , mm	Type of pipe
3	0.77	0.44	2247	B
3	0.50	0.44	2433	B
3	1.02	0.44	2247	C
3	0.65	0.44	2433	C
5	1.15	0.51	2247	B
5	0.62	0.51	2433	B
5	Not lifted	–	2247	C
5	0.84	0.51	2433	C

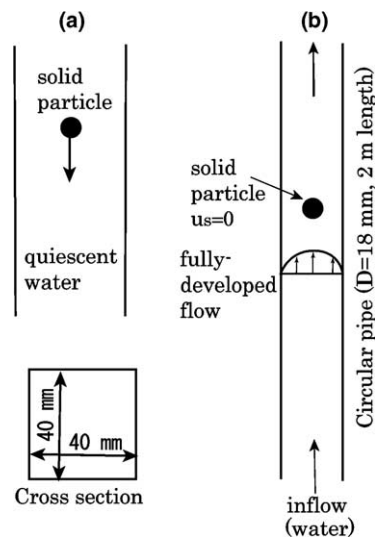


Fig. 7. Experimental setup for measuring terminal velocity (a), and for measuring critical water flux for conveying a solid particle in a fully developed flow (b).

For comparison, the authors also examined the critical water flux for transporting a solid particle in a fully developed steady flow in a vertical straight pipe as shown in Fig. 7(b). The pipe diameter and height were 18 mm and 2 m, respectively. First, water in the pipe was quiescent and a solid particle was set at the bottom of the vertical pipe. Water was then introduced into the bottom of the pipe, creating forced upward water flow. The flow rate was increased gradually until the particle began to ascend. By adjusting the water flow rate, it was possible to determine the critical conditions for which a solid particle remained stationary at approximately 1.5 m away from the bottom of the pipe (where the flow is regarded as fully developed). During these measurements, the particle remained near the center axis of the pipe. The measured critical water flux in a fully developed flow was $j_L = 0.43$ m/s for $d_s = 3$ mm, and $j_L = 0.49$ m/s for $d_s = 5$ mm, respectively. These values were very close to those of three critical water flux, $j_{L,min}$, for the air-lift pump, though the fully developed steady flows differed from the unsteady flows in the air-lift pump. This fact might suggest that the time-averaged radial velocity profile in the air-lift pump is similar to that for a fully developed flow.

The critical flux for a fully developed flow also differed from the terminal velocity, due to the radial velocity profile of a fully developed flow in the circular pipe. The water flux (or superficial velocity) is regarded as the mean velocity over the circular cross-section. As the Reynolds number (based on the mean velocity and the inner pipe diameter) is 7740 and 8820 for $d_s = 3$ and 5 mm, respectively, the radial velocity profile is approximated by the 1/7th power law. Therefore, the fluid velocity at the center axis must be at least 20%

larger than the mean velocity, explaining why the critical flux for the fully developed flow is smaller than the terminal velocity.

Based on the measurements of the critical condition for a single particle, the performance curves for three-phase mixture in Fig. 5 are examined again. It is apparent that the solid particles are lifted if the water flux is greater than the critical value, $j_{L,\min}$. In several cases, particles are transported by a water flux less than the critical value determined as necessary for lifting a single particle. The reason will be discussed in later subsection. In addition, the particles are not conveyed for the cases of $L_s = 1925$ mm, where the maximum water flux is lower than the critical value for both 3 and 5 mm diameter of a single particle. From the results, the critical condition for lifting a single solid particle or that for a fully developed flow is a useful index to roughly predict the possibility of transporting solid particles in air-lift pumps.

3.3. Photographic observations of particle motion in S-shaped section

Particle motion in the region of a pipe bend was investigated through photographic observations to understand the physics of phenomena occurring in the air-lift pump. Fig. 8 shows photographs of the distribution of particles in the horizontal pipe region for pipe B, $L_s = 2247$ mm, and $j_s = 0.002$ m/s. The conditions of pump operation (i) to (iii) correspond to the same symbols indicated in Fig. 5(a). Although the discharged particle flux is the same for all cases, the number density of solid particles in the figure is obviously different. In

case (i), the number of particles is low. The drag force exerted from water flows is dominant to the particle motion, while the gravitational force is insignificant in the horizontal section. Only the friction between pipe wall and solid particles reduces the moving velocity of particles. Thus, particles roll smoothly from right to left on the lower side of pipe wall. Since the water flows are essentially unstable and the particles give rise to complex liquid wake flows behind themselves, the number density of solid particles is changeable locally as well as temporarily.

In case (ii), where the discharged water flux is close to the critical value, the number of particles in the horizontal pipe region is larger than that in case (i), and smaller than in case (iii). Also, the local velocity of liquid phase is small compared to case (i), because the discharged water flux is small. A string of particles moves slowly along the pipe wall. As a consequence, the number density of particles is approximately uniform in the horizontal section.

In case (iii), where the discharged water flux is less than critical, many particles reside in the horizontal region of the pipe. Most of them are almost stagnant. Local velocity of them is very small. Relatively few particles move on a bed of stuck particles. The flow area for liquid phase becomes small because of the presence of stuck particles. The shape of interface between the bed of stuck particles and the liquid becomes somewhat wavy due to unsteady liquid flows.

Fig. 9 shows photographs of particle motion at a bend. The experimental conditions coincide with those in Fig. 8. In case (i), some colonies exist where the number density of particles is high. In cases (ii) and (iii), many solid particles are observed in the pipe-bend region. The motion of particles is very complicated and unsteady in all cases. Many particles are seen in the lower/outer part of the circular cross-section of the pipe. They are moving in upward or downward. The number density of particles is relatively small in the upper/inner part of cross-section. The particles in the region have trends to move in upward. Relatively few particles reach the upper part (gas injector).

To investigate such complicated particle motion quantitatively, the track of individual particle is followed using a video camera. Fig. 10 represents the time evolution of location of two solid particles at every 0.1 s for pipe B, $L_s = 2247$ mm, and $j_s = 0.003$ m/s. It is noted that the positions of particles directly measured from the video images. As the light refraction occurs at curved air/glass or glass/water interfaces, the plotted data in the figure do not necessary mean spatially exact particle tracks. The particle motion is very similar to that in case (ii) or (iii), although the experimental conditions are different. One particle indicated by black circles in the figure is almost stagnant in the horizontal section after it was trapped in a bed of stuck particles. Another particle

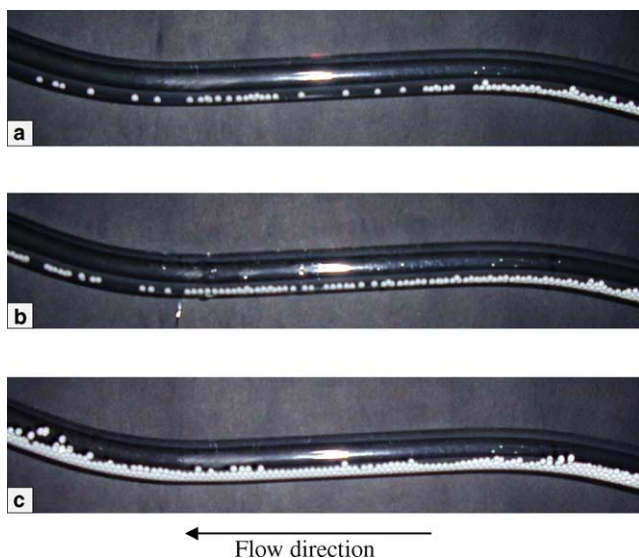


Fig. 8. Instantaneous photographs showing particle motion in the horizontal pipe region for $L_s = 2247$ mm, $d_s = 3$ mm, pipe B, and $j_{Ga} = 1.96$ m/s (a), $j_{Ga} = 3.27$ m/s (b), $j_{Ga} = 1.31$ m/s (c).

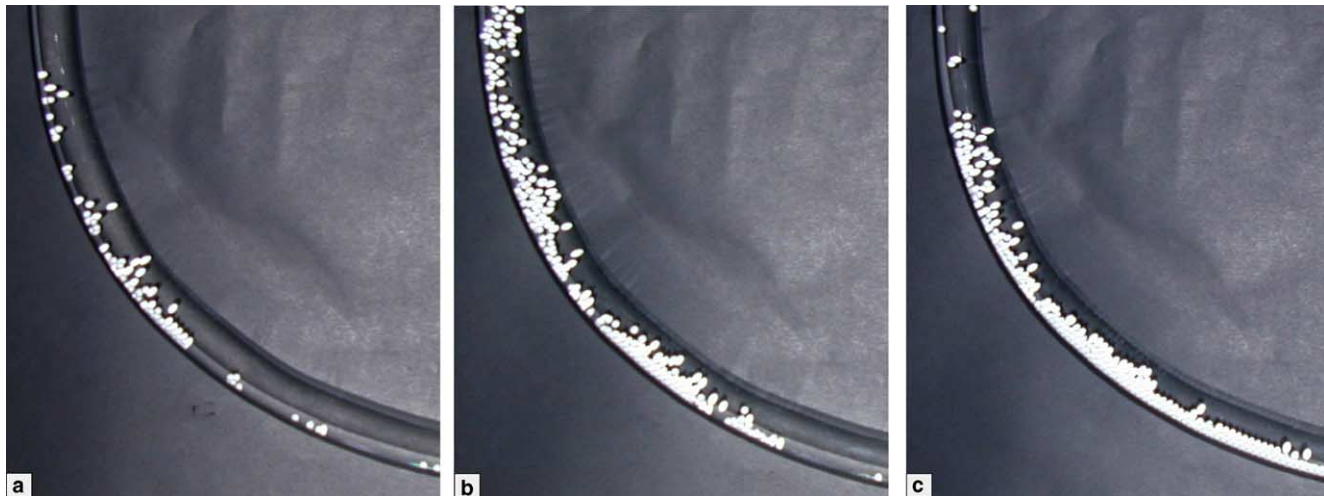


Fig. 9. Instantaneous photographs showing particle motion in the pipe-bend region for $L_s = 2247$ mm, $d_s = 3$ mm, pipe B, and $j_{Ga} = 1.96$ m/s (a), $j_{Ga} = 3.27$ m/s (b), $j_{Ga} = 1.31$ m/s (c).

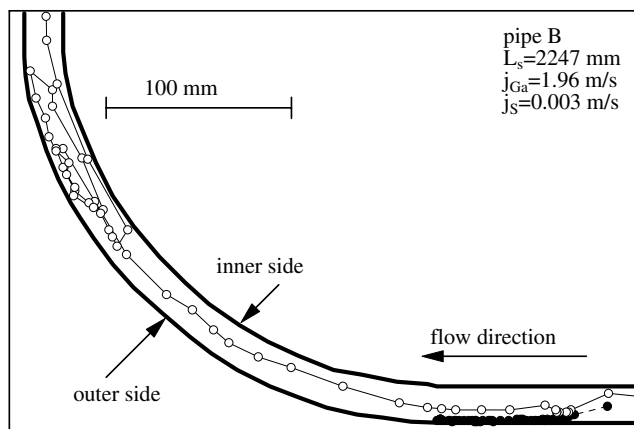


Fig. 10. Time evolution of location of particles for $j_{Ga} = 1.31$ m/s, $j_s = 0.003$ m/s, $L_s = 2247$ mm, and pipe B.

shown by white circles moves on a bed of stuck particles in the horizontal section and then goes up in the pipe-bend region. Judging from the distance between every successive two positions of the particle, the velocity of particle is changeable temporarily as well as locally, due to unsteady nature of the flows. The particle reaches a certain vertical point in the bend section, slows down, moves outward, and then falls down slowly along the outer wall of the pipe where the number density of particles is large. The particle goes up and down for a while at relatively small velocity. Subsequently, the particle moves inward and then ascends. The local velocity of the particle is apparently small if it is in the region of outer part of cross-section of the pipe. On the other hand, the local velocity of the particle located in the inner side is relatively high. This fact indicates that the local liquid velocity is high in the inner side of cross-section of the pipe.

It should be noted that the mean velocity of the mixture of water and air becomes much higher above the gas injector, because the volume fraction of air is considerably large. Thus, the particles are transported easily in the three-phase region compared to the water–solid particles two-phase region.

The reason why the particles are transported despite the water flux being less than critical is due to the large number density of particles. This leads to a locally smaller flow area for the liquid phase, and the liquid velocity becomes locally as well as temporarily higher than the critical velocity. As a result, only some limited particles are lifted upward. Such flow is unsuitable from a practical viewpoint, since there is a high possibility of particle clogging. In actual use, the air-lift pump should not be operated just above the critical conditions for lifting a single particle.

The mixture of air–water–solid particles flows in the pipe-bend region when the gas injector is set below the S-shaped pipe. Fig. 11 depicts photographs showing the flow motion in pipe C for $L_s = 2433$ mm. The experimental condition corresponds to case (iv), as indicated in Fig. 5(e). Since lights are reflected at the air–water interfaces, the photographs are quite unclear. But it is apparent that the air and the water flow separately in the horizontal pipe region: the air flows in the upper part of the pipe, while the water flows in the lower part. In this case, the discharged water flux is greater than the critical value. Furthermore, the local water velocity in the three-phase region is much larger than the superficial velocity of water (water flux), because the volumetric fraction of air is appreciably large. As a consequence, particles are transported quickly. The particles reside in the lower part in the horizontal section due to their large material density. In the bend section, most of particles move in the outer part of cross-section of the pipe, because of particle inertia.

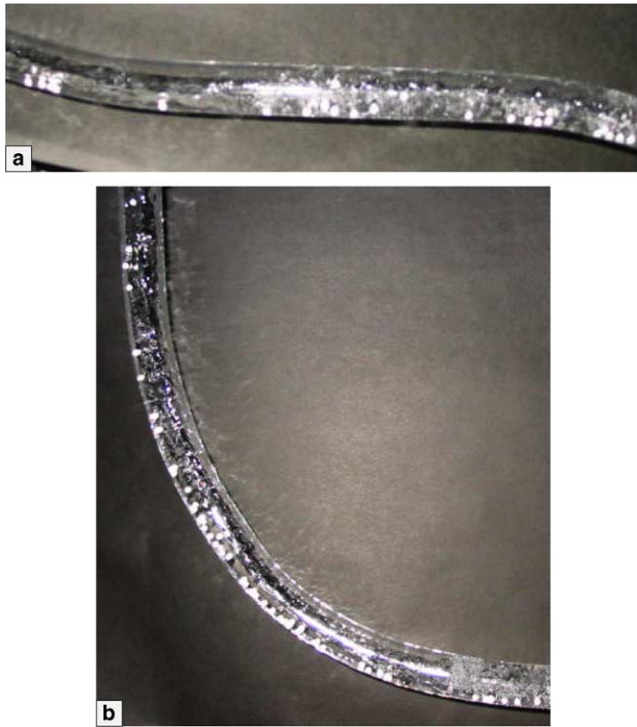


Fig. 11. Instantaneous photographs showing particle motion in the horizontal pipe region (a) and the pipe-bend region (b) for $j_{Ga} = 1.96$ m/s, $L_s = 2433$ mm, $d_s = 3$ mm, and pipe C.

4. Conclusions

The pump performance of locally bent air-lift pumps for conveying solid particles was investigated experimentally. The main results obtained by the present study are listed below.

The presence of pipe bends reduces the pump performance. If the pipe bend is set below the gas injector, the reduction in pump performance is small. However, when the pipe bend is set above the gas injector, appreciable reduction of pump performance occurs. Pipe bends should not be set above the gas injector.

Three types of critical condition for transporting a solid particle were measured: the terminal velocity of a solid particle in a quiescent fluid, the critical flux for a steady fully developed pipe flow, and the critical flux for the air-lift pump. The critical conditions for the latter two agreed well.

The water flux for three-phase flows is essentially less than that for the case of two-phase flow. The water flux

at a given gas flux decreases with increasing flux of solid particles. The solid particles will be lifted if the water flux is larger than the critical value, $j_{L,min}$.

It is found that the solid particles will be conditionally lifted, even if the water flux is less than $j_{L,min}$, because of reduction of water flow area by large number density of particles. In actual use, the air-lift pump should be operated under the condition that the discharged flux is higher than the critical one for lifting a single particle to avoid particle clogging.

The motion of particles in the horizontal pipe section or the pipe-bend region is very complicated in nature. The particle velocity is changeable locally as well as temporarily, depending on unsteady liquid flows.

Acknowledgements

The authors would like to thank Mr. Takuya Nagatani, who is an undergraduate student at Kyoto University, for his faithful help in the experiments.

References

- Fujimoto, H., Ogawa, S., Takuda, H., Hatta, N., 2003. Operation performance of a small air-lift pump for conveying solid particles. *Trans. ASME J. Energy Res. Techn.* 125, 17–25.
- Hatta, N., Omodaka, M., Nakajima, F., Takatsu, T., Fujimoto, H., Takuda, H., 1999. Predictable model for characteristics of one-dimensional solid–gas–liquid three-phase mixtures flow along a vertical pipeline with an abrupt enlargement in diameter. *Trans. ASME J. Fluids Eng.* 121, 330–342.
- Kato, H., Miyazawa, T., Tiyama, S., Iwasaki, T., 1975. A study of an air-lift pump for solid particles. *Bull. JSME* 18 (117), 286–294.
- Khalil, M.F., Elshorbagy, K.A., Kassab, S.Z., Fahmy, R.I., 1999. Effect of air injection method on the performance of an air lift pump. *Int. J. Heat Fluid Flow* 20 (6), 598–604.
- Sekoguchi, K., Matsumura, K., Fukano, T., 1981. Fluctuation characteristics of a natural circulation air-lift pump (Part 1). *Trans. JSME* 47 (415), 484–492.
- Shaw, J.L., 1993. Nodule mining—three miles deep!. *Marine Georesour. Geotechnol.* 11, 181–197.
- Weber, M., Dedegil, M.Y., 1976. Transport of solids according to the air-lift principle. In: *Proc. 4th Int. Conf. on the Hydraulic Transport of Solids in Pipes*, Alberta, Canada, H1-1-23 and X93-94.
- Yoshinaga, T., Sato, Y., 1996. Performance of an air-lift pump for conveying coarse particles. *Int. J. Multiphase Flow* 22, 223–238.